Pilot facility for the study of thermal energy storage: Experiments and Theoretical model

A. Castro-Vizcaíno[1,2], K. Babul[3], M.S. Romero-Cano[1,2], J.L. Bosch[1,2], M.J. Ariza[1,2], J. Alonso-Montesinos[1,2], A.M. Puertas[1,2], B. Gil[4], S. Rosiek[4]

[1] Department of Chemistry and Physics, University of Almería, Ctra. Sacramento s/n, Almería, 04120, Spain

[2] CIESOL, Joint Centre of the University of Almería-CIEMAT, Ctra. Sacramento s/n, Almería, 04120, Spain

[3] Department of Energy Conversion Engineering, Wroclaw University of Science and Technology, Wybrzeze Wyspianskiego 27, Wroclaw, 50370, Poland

[4] Department of Thermodynamics and Renewable Energy Sources, Wroclaw University of Science and Technology, Wybreze Wyspianskiego 27, Wroclaw, 50370, Poland

Abstract

Thermal energy storage is a widely used solution to address the mismatch problems between energy availability and demand. However, research in this topic is still necessary to optimise the benefits of energy storage. For this purpose, many research groups have designed and built pilot facilities that allow the study of small pilot tanks for further optimization of storage parameters. Here, we present an experimental setup to study the charging and discharging of thermal energy in a storage tank intended for refrigeration. The facility consists of a chiller which cools down the heat transfer fluid (water/glycol mixture), an 80-litres inertia bath to enhance the chiller's cooling capacity, and a storage tank of 60 litres. A three-way valve allows to control the inlet storage tank temperature, and an electric heater is used with the purpose to study the tank discharging process. A theoretical model representing the energy balance equations for each pilot's components is also presented to rationalise the experimental results. The model reproduces satisfactorily the operation of the system and shows that even minimal thermal losses must be accounted for. Finally, the energy stored in the tank is calculated, showing that up to 30% of the inlet energy is dissipated to the environment, which was also represented by the developed theoretical model.

Keywords: Thermal energy storage, pilot facility, thermodynamic modelling

1. Introduction

The demand of energy for the development of our societies is continuously increasing during the last few decades, while this is in stark contrast with the necessity to reduce gas emissions. This combination has been the driving force for research in renewable energies and energy storage. Buildings is one of the sectors where the demand is increasing more rapidly, amounting to 132 exajoules in 2021, around 30% of the global energy consumption, according to the REN21 Global Status Report (Ren21, 2023), and around 75% of this demand is used for space heating and cooling. However, only 14% of the heating demand was covered with renewable energy in 2021, mainly due to the intermittency of the energy source and the mismatch between energy production and demand, in comparison to the easiness and fastness of fossil fuels-based technologies. Nevertheless, thermal energy storage is perfectly suited to cover this mismatch (Cabeza, 2022; Lizana, 2018).

Several strategies have been developed, but the most widely extended ones are storing the thermal energy in the form of temperature variations of a substance (sensible heat) or inducing a phase change in a so-called phase change material, PCM, (Alva, 2018). Although the use of thermal energy storing is common in many different applications, there are many aspects that need further research, such as the internal structure of the tanks, the control strategies, or the development of new materials. For this purpose, many researchers have designed pilot plants that allow the study of small storage systems. The analysis of the results from these

10.18086/eurosun.2024.06.03 Available at http://proceedings.ises.org

experiments is then up scaled into real applications, but this requires a deep understanding of the pilot facility. For instance, Koukou et al. (Koukou, 2020) built a prototype storage system based on PCMs, and with two different energy sources, solar and geothermal energy. Two different PCMs were tested, and the most stable output is proposed as optimal for their application. Weiss et al. (Weiss, 2021) studied numerically the stratification inside a tank to conclude that the idealised flow distribution misestimated the thickness of the thermocline and optimised the inlet location for their application. In refrigeration applications, Selvnes et al. (Selvnes, 2021) designed and tested a novel plates-in-tank storage unit, integrated in a pilot facility modelling industrial refrigeration systems based on CO_2. Even more, the combination of modelling and experiments improves the understanding of an actual facility, in particular for the analysis of heat losses in a storage tank, as performed by Mawire (Mawire, 2013). These few examples show that this field is still under development, mainly due to the many different processes involved in it.

In this work, we present a pilot facility for the study of a storage tank of 60 litres, aimed for the analysis of PCMs as storage medium for refrigeration (the whole system operates at sub-zero temperatures). It is composed of a chiller unit and a buffer, or inertia, bath of 80 litres, a heater, and the storage tank. In the present work and with the main goal to simplify the experiments, the storage tank does not contain PCMs, and only the heat transfer fluid (HTF) is used as storage medium. The system allows setting the mass flow rate and storage inlet temperature, as well the heater to simulate an external load to activate the tank discharging process. Moreover, a theoretical model is also presented, based on the energy balance of the main components of the facility, where most of the parameters are taken from the real experiment. The comparison of the model with the experiments shows that even minimal thermal losses must be considered in the storage design process, therefore its importance when we compare to the total energy stored in the tank were also presented.

This work is part of the European Life Programme project COOLSPACES 4 LIFE, aimed to test the viability of thermal PCM-based energy storage for a newly developed solar powered air conditioning system.

2. Materials and methods

2.1. Technical data

Figure 1 illustrates the pilot unit of the cooling system, which includes the inertia tank, an electric heater, two circulation pumps, two and three-way valves, and its corresponding piping. Panels (b) and (c) present the storage tank from side and top views, respectively. A glycol/water mixture (70/30) has been used as the heat transfer fluid (HTF). The cooling unit, has a cooling capacity rating of 1.7 kW and operates on a conventional vapour-compression refrigeration cycle. This is composed of a compressor, a condenser, an expansion valve, and an evaporator, along with the R449A refrigerant gas. Its temperature operating range varies from -40 ºC to +100 ºC and can withstand pressures up to 28 bars. The buffer tank has a storage capacity of 80 litres. An electric heater, is used to activate the storage tank discharging process, and has a power of up to 2 kW. The circulation pumps allows variable flow rates, varying the electricity power from 18 W to 191 W. The inertia tank and all conducting pipes are thermally isolated with a elastomeric insulating foam.

The right section of the experimental setup (c.f. Fig.1 c) presents a horizontal thermal storage tank that was designed for sensible or latent heat storage. This work focuses only on sensible heat storage operation conditions, while latent heat storage experimental results will be presented in the near future. The presented storage tank was designed within the COOLSPACES 4 LIFE project and manufactured by one of consortium partner Hedera Helix. Constructed from stainless steel, the tank's dimensions are 750 mm x 400 mm x 200 mm, with a total volumetric capacity of 60 litres. It is equipped with small observation windows to monitor the fluid dynamics. For precise temperature control, six holes have been integrated in one side of the tank, facilitating the insertion of six probe branches with racor connections to prevent HTF leaks. This design allows the accommodation of up to 32 probes. To mitigate fluid stratification, the tank incorporates eight fluid inlets, four at the upper level and four at a level immediately below, with an equivalent configuration at the tank outlet. An access gate is installed at the top of the tank, enabling the manipulation of internal probes and encapsulated phase change materials (EPCMs) for future experimental applications. Thermal insulation is provided by an external layer of polyurethane insulating foam surrounding the whole tank, except the observation windows and gate.

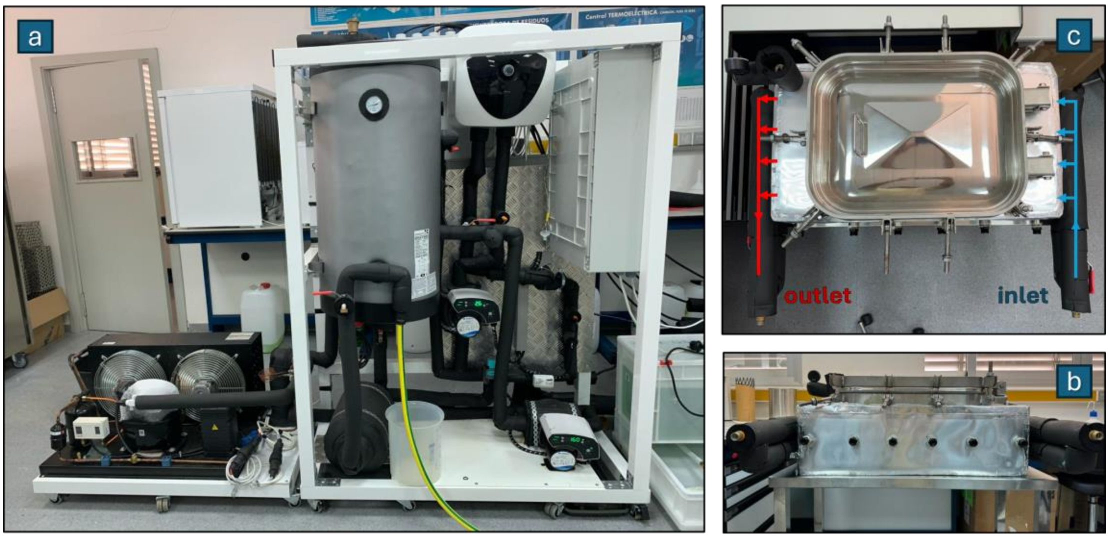

Fig. 2.1: Photograph of the experimental cooling setup with the buffer tank and the heater on the left and a top view of the horizontal storage tank on the right (c) along with a front view (b).

2.2. Operation mode

The presented in this work experimental set-up can operate in two different modes: charging mode, extracting heat from the storage tank, then cooling it down, as well discharging mode, where the cold fluid stored in the tank is circulated through an electrical resistance which simulates a constant energy demand. Thanks to that we can use this prototype for scaling up to a real storage system application in the air-conditioning building systems. Both operational modes are described in greater detail below:

Charging Mode:

This mode starts with the pre-cooling of the heat transfer fluid (HTF) that circulates through the entire system. This cooling is achieved by a heat exchanger in the chiller unit (refrigerant gas-glycol mixture), specifically the evaporator of the cycle. As the HTF cools, (negative) energy is accumulated in the buffer tank until it reaches the set point (T_{buffer}). Once the buffer tank is charged, the actual charging of the thermal storage tank begins, using the energy stored in the buffer tank while the chiller tries to keep its temperature to the set point. The temperature of the inlet to the storage tank (T_{inlet}) is fixed (above the temperature of the inertia bath) using the three-way valve, mixing the outlet of the storage and buffer tanks. This operational mode is designed to minimise the charging time. A hysteresis mechanism is used in the buffer tank to allow variations of the temperature around the set point without the chiller working.

Discharging Mode:

When the thermal storage tank is cold charged, it can be discharged using the heater. This operation mode involves circulating the HTF against a variable load resistance (fixed load during each test), thereby dissipating all the stored energy during the charging process and simulating a real discharging operation.

For both operation modes, the parameters that the user can modify include: buffer tank temperature, inlet temperature to the storage tank, system flow rate, power of the general pump, opening or closing of the three-way valve and the percentage of load offered by the resistance. The system flow rate is controlled by the power of the general pump and the two-way valve located at the storage tank outlet, which operates automatically based on the integrated control system. To control the inlet temperature to the storage tank, the three-way valve operates freely to regulate the water mixture between the storage tank outlet and the buffer tank outlet, thereby adjusting the temperature to the selected set value. When the system operates in discharging mode, the valve must be closed to 0% to prevent the controller from acting and to maintain HTF recirculation through the resistance without mixing the fluid with the buffer tank.

3. Model description

In order to model the experimental setup described previously, it is schematized as shown in Fig. 3.1. The approximation of subcooled liquids is used, where the change in enthalpy is written as $\Delta h = c_p \cdot \Delta T$ in the energy balance equation:

$$\frac{dE_{vc}}{dt} = \dot{Q} - \dot{W} + \sum_e \dot{m}_e h_e - \sum_s \dot{m}_s h_s \quad (1)$$

where E_{vc} stands for the energy in the control volume, $\dot{Q}$ and $\dot{W}$ correspond the heat and work exchanged through the boundaries, and $\dot{m}$ is the mass flow rate. The subindices e and s refer to "entering" and "leaving" the control volume.

Only the heat exchanger of the cooling unit is considered, with a cooling capacity $\dot{Q}_{cooler}$. Ideal mixing is assumed in both the *inertia bath* and the *storage tank*, and heat losses are assumed, proportional to the temperature difference with the ambient. The three-way valve is also included, with a control similar to the experimental setup, to achieve the target temperature entering the *tank*, T_{3a}. The heater is active only in the discharging mode and is characterised by the thermal power $\dot{Q}_{heater}$.

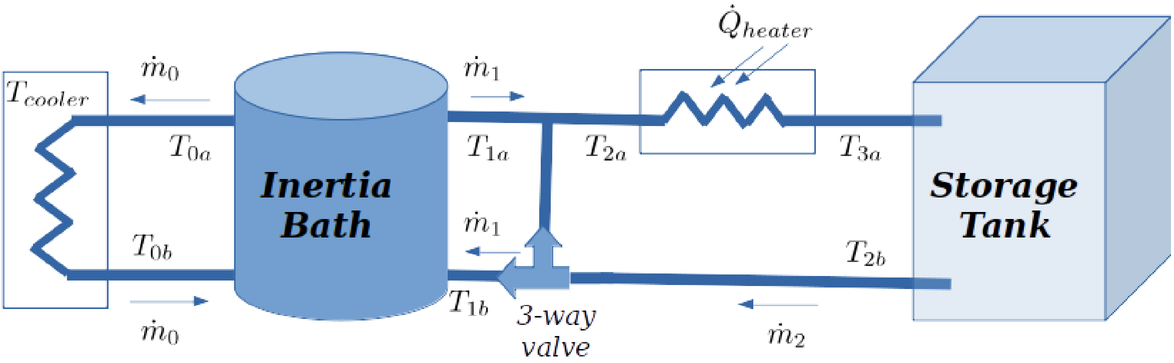

Fig. 3.1: Schematic representation of the experimental setup, with the variables for the model

The governing equations are therefore as follows:

- Cooler. The heat released by the refrigerant, at temperature T_{cooler}, is given by $\dot{Q}_{cooler} = k(T_{cooler} - T_{0a})$, where k is a heat transfer coefficient to be determined. Assuming that the cooler is in the stationary state, the temperature of the HTF leaving the cooler is:

$$T_{0b} = T_{0a} + \frac{k}{\dot{m}_0 c_{HTF}}(T_{cooler} - T_{0a}) \quad (2)$$

  with c_{HTF} the specific heat capacity of the HTF.

- Bath. The inflows with temperatures T_{0b} and T_{1b} mix, and the temperature of the outlets are equal, and identical to the bath temperature: $T_{0a} = T_{1a} = T_{bath}$. This is calculated as:

$$\frac{dT_{bath}}{dt} = \frac{\dot{m}_0}{m_{bath}}(T_{0b} - T_{bath}) + \frac{\dot{m}_1}{m_{bath}}(T_{1b} - T_{bath}) + \frac{\dot{Q}_{env}}{m_{bath} c_{HTF}} \quad (3)$$

  where m_{bath} is the HTF mass inside the bath. The heat loss to the environment is calculated as:

$$\dot{Q}_{env} = k_{env}(T_{bath} - T_{env}) \quad (4)$$

  with k_{env} a constant that controls the heat exchange.

- 3-way valve. This is used to fix the temperature T_{3a} in the charging mode. The opening of the valve is calculated as:

$$x_v = \frac{T^*_{tank} - T_{tank}}{T_{bath} - T_{tank}} \tag{5}$$

where T^*_{tank} is the set point of the tank; when x_v, calculated with this equation is larger than one, it is set to one. The mass flow rate entering the inertia bath from the storage tank is then set according to $\dot{m}_1 = x_v \cdot \dot{m}_2$.

In the discharging mode, in contrast, x_v is fixed $x_v = 0$, and the heater is connected.

- Heater. To model the electric resistance, only the heat flux to the HTF is considered:

$$T_{3a} = T_{2a} + \frac{\dot{Q}_{heater}}{\dot{m}_2 c_{HTF}} \tag{6}$$

where $\dot{Q}_{heater}$ is the heat transferred to the HTF per unit time, which is assumed to be equal to the power of the electric resistance.

- Storage tank. This reservoir is intended to store the energy, either using sensible heat (with HTF or another material), or latent heat with PCM; in our case, energy is stored in the HTF. The energy balance in the tank results in:

$$\frac{dT_{tank}}{dt} = \frac{\dot{m}_2}{m_{tank}}(T_{3a} - T_{tank}) + \frac{\dot{Q}_{env}}{m_{tank} c_{HTF}} \tag{7}$$

where the heat gain from the environment is calculated as in eq. (4), with the tank temperature instead of the bath temperature. The parameter k_{env} is similar in both cases, for simplicity, and is expected to be very small.

The system of equations formed by equations (2), (3), (4), (6), and (7) with the relation between the mass flow rates with x_v, is solved numerically, obtaining the evolution of all temperatures as a function of time, and allowing a direct comparison with the experiments. This requires the specification of T_{cooler}, k and k_{env}, which cannot be accessed experimentally, whereas the flow rates, mass of HTF in the bath, and power of the heater are taken from the experimental setup. The time step is set to δt = 1s, which was checked to be small enough not to influence the results.

4. Results

Fig. 4.1 shows the results of a single experiment and its comparison with the theoretical model presented in previous section. The initial part of the graph (for time below 150 min) shows the cooling of the inertia bath, until it reaches -8 ºC. At t = 150 minutes, the HTF is directed to the storage tank, while the primary loop keeps cooling the bath, as far as it is above the set point (-7 ºC with a hysteresis of 1.25 ºC in this experiment). At t = 300 minutes, the tank has been fully charged as noted by the outlet temperature, which is constant, and discharging process starts with the heater, with a power set to 2000 W. The 3-way valve is closed, and the inlet temperature raises notably.

The predictions of the model, without heat losses, are shown in Fig. 4.2, with T_{cooler} = -13 ºC and $k = 100\ W\ K^{-1}$. These parameters control the initial kinetics, i.e. the charging of the inertia bath, and only k_{env} remains to be determined, while all other parameters are taken from the experiment, including the operation times. At t = 150 min. the cold HTF from the bath is directed to the storage tank, and it charges until the inlet and outlet temperatures are equal. In this case, heat losses are not considered, $k_{env} = 0$, and the inertia bath keeps its temperature when the storage tank is fully charged. This disagrees with the experiments of Fig. 4.1, where the inertia bath heats up slowly as soon as the cooler is disconnected.

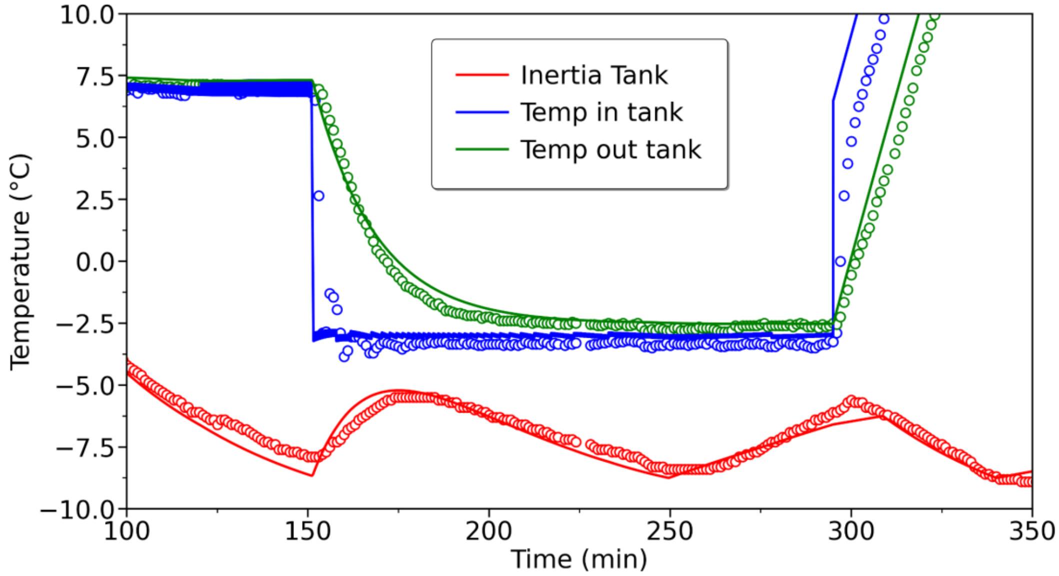

Fig. 4.1: Experimental evolution of the temperature in the inertia bath (red line), inlet and outlet to the storage tank (blue and green lines, respectively).

Therefore, heat losses must be included in the model, and the lines in Fig. 4.1 show the results for $k_{env} = 0.00125\, W\, K^{-1}$, which agree with the experiments (all other parameters are equal to the previous case). Notably, the value of the heat transfer coefficient is much smaller for the heat losses than for the heat exchanger in the cooler, as expected from the isolation of the pipes and reservoirs. It is interesting to note also that the outlet from the tank is in this case always slightly hotter than the inlet. The comparison of these results with Fig. 4.2 shows that heat losses, although minimal, are indeed relevant in the experimental system design, and the model provides an appropriate description of the processes involved in the operation of the experimental set up.

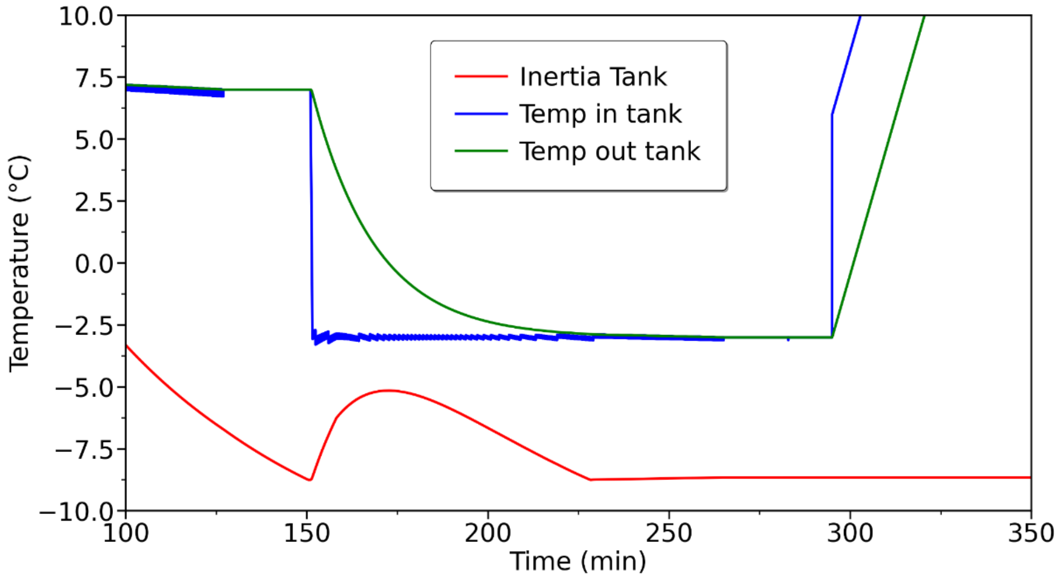

Fig. 4.2: Evolution of the temperature in the inertia bath (red line), inlet and outlet to the storage tank (blue and green lines, respectively) in the model, without heat losses.

On the other hand, when we analyze the energy stored in the tank, we can calculate the energy balance in the tank with the temperature of the inlet and outlet flows. In particular, for the storage tank, the total (negative) energy driven into tank is calculated as below:

$$E_{vc} = \int_{t_0}^{t_1} dt\, \dot{m}\, c_{HTF}(T_{3a} - T_{2b}) \tag{8}$$

A fraction of this energy is stored in the tank, whereas the rest is transferred to the environment (actually, because the energy is negative, the energy is gained from it).

Fig. 4.3 shows the evolution of the energy (in absolute value) for the same case as presented above, comparing the experiments and simulations. The horizontal line shows the energy that can be stored according to the change of HTP temperature:

$$Q = m_{tank} c_{HTF} \Delta T \tag{9}$$

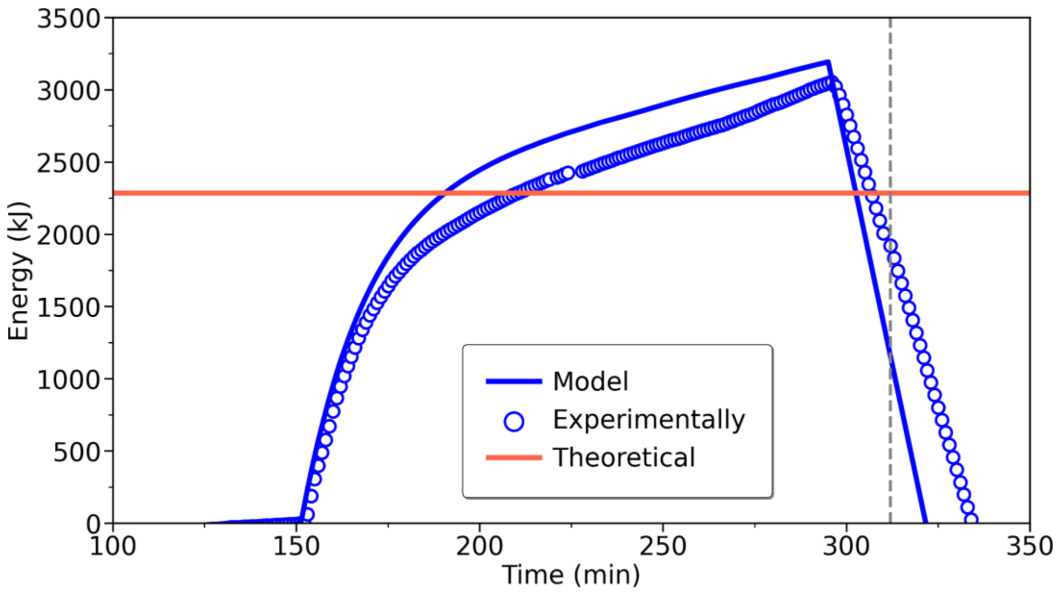

Fig. 4.3: Energy transferred into the storage tank, experimentally (circles) and from the model (line). The horizontal line represents the energy stored in the HTF according to eq. (9).

After the tank has been charging for 150 minutes, it is discharged with the heater, as mentioned above, and the energy in the tank starts decreasing. After 20 minutes, the outlet temperature reaches the initial temperature of the storage tank, 7 ºC (marked by the vertical line) in the figure. The difference between the energy when the discharging starts, and this point, is the energy that could be recovered in this experiment, which, in principle, should agree with the stored energy (horizontal line in the figure).

Fig. 4.4 shows the energy driven to the storage tank, calculated from the experiment and model, with the calculation of the sensible energy in the HTF, eq. (9), and the energy recovered experimentally during the discharging phase. This graph shows that in the model and experiments a large fraction of the energy introduced in the tank is dissipated to the environment, up to 30% in the experiments and up to 25% in the model, whereas the fraction of recovered energy is below the estimated store energy. Notably, the model and experimental results follow the same trend, with small quantitative differences between them.

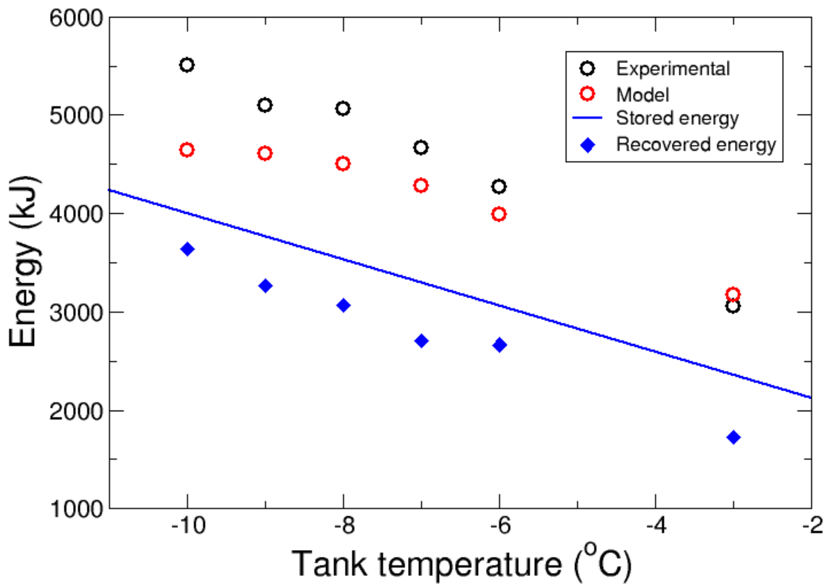

Fig. 4.4: Energy transferred into the storage tank, experimentally (black circles) and from the model (red circles), as a function of the set point tank temperature. The line represents the store capacity according to eq. (9), and the blue diamonds show the energy that is recovered.

5. Discussion and conclusions

Although the model presented here is very simple, and contains only a limited number of parameters, it provides an acceptable description of the presented pilot facility through the evolution of the temperatures in key locations, and the subsequent analysis of storage tank energy balance. Even more, it has led us to verify and quantify the heat gains from the environment that are necessary for a full interpretation of the experimental results. The prototype is now well understood, with all relevant parameters characterised properly, thus the model can be used to predict its behaviour in different circumstances.

In summary, we have presented a prototype cooling facility connected to a tank intended for thermal energy storage for refrigeration. A model describing the thermal balance of each its component has been used to rationalise the results, with a small number of adjustable parameters. The model has shown that thermal losses, although minimal, are relevant to interpret correctly the experimental results, allowing to calculate with good agreement between experiments and the model the amount of energy stored in the tank, and dissipated to the environment.

An attractive future work could consist of EPCMs introduction in this pilot storage tank to perform charging and discharging cycles with the main goal to gain knowledge for full scale tank operation, that are going to be installed in two institutional buildings in different locations: Almeria (Spain) and Wroclaw (Poland).

6. Acknowledgments

The COOLSPACES 4 LIFE project (LIFE20 CCM/PL/001607) is financed by the European Commission under the LIFE Programme and co-financed by the National Fund for Environmental Protection and Water Management in Poland (Project 2244/2021/WN01/OA-PO-LF/D).

Sabina Rosiek is most grateful for the financial support from the Polish National Agency for Academic Exchange, Polish Returns 2018 (https://nawa.gov.pl/en/), with the project identification number: 07PP/0001/19.

7. References

Alva, G., Lin, Y., Fang G., 2018. An overview of thermal energy storage systems. Energy, 144, 341-378.

Cabeza, M.L. (ed.), 2022. Encyclopedia of Energy Storage (four volumes). Elsevier. (See in particular the first volume for Thermal Energy Storage).

Koukou, M.K., Dogkas, G., Vrachopoulos, M.Gr., Konstantaras, J., Pagkalos, Ch., Stathopoulos, V.N., Pandis, P.K., Lymperis, K., Coelho, L., Rebola, A., 2020. Experimental assessment of a full scale prototype thermal energy storage tank using paraffin for space heating application. International Journal of Thermofluids, 1-2, 100003.

Lizana, J., Chacartegui, R., Barrios Padura, A., Ortiz, C., 2018. Advanced low-carbon energy measures based on thermal energy storage in buildings: A review.Renewable and Sustainable Energy Reviews, 82, 3705-3749.

Mawire, A., 2013. Experimental and simulated thermal stratification evaluation of an oil storage tank subjected to heat losses during charging. Applied energy, 108, 459-465.

REN21,2023. Renewables 2023 Global Status Report collection, Renewables in Energy Demand. ISBN 978-3-948393-07-6.

Selvnes, H., Allouche, Y., Hafnes, A., 2021. Experimental characterisation of a cold thermal energy storage unit with a pillow-plate heat exchanger design. Applied Thermal Engineering, 199, 117507.

Weiss, J., Ortega-Fernández, I., Müller, R., Bielsa, D., Fluri, Th., 2021. Improved thermocline initialization through optimized inlet design for single-tank thermal energy storage systems. Journal of Energy Storage 42, 103088.